A structural, magnetic and Mössbauer investigation on melt-spun $Nd_{0.33}(Fe_{0.75}Al_{0.25})_{0.67}$ ribbons

1999 J. Phys.: Condens. Matter 11 10557

(http://iopscience.iop.org/0953-8984/11/50/341)

J. Phys.: Condens. Matter **11** (1999) 10557–10566. Printed in the UK PII: S0953-8984(99)05760-4

A structural, magnetic and Mössbauer investigation on melt-spun $Nd_{0.33}(Fe_{0.75}Al_{0.25})_{0.67}$ ribbons

L Si, J Ding, Y Li, L Wang and X Z Wang
Department of Materials Science, National University of Singapore, Singapore 119260

Received 6 July 1999

Abstract. A tetragonal phase with $a = 9.778$ Å and $c = 11.516$ Å is formed in the $Nd_{0.33}(Fe_{0.75}Al_{0.25})_{0.67}$ alloy after melt spinning and short period annealing at 873 K. The tetragonal phase is probably metastable and transforms slowly into the stable δ-$Nd_3Fe_{7-x}Al_x$ phase during heat treatment at 873 K. This phase is antiferromagnetic with a Néel temperature of 260 ± 5 K. Metamagnetism is observed at a temperature of 140 K or below. The magnetic properties have been characterized using a vibrating sample magnetometer and Mössbauer spectroscopy. Magneto-resistivity of up to 7.2% is accompanied by metamagnetism. At room temperature, 1% of the magneto-resistivity is measured in the paramagnetic state.

1. Introduction

Rare-earth (RE) and transition metal compounds possess many unique magnetic properties and they are widely found in many applications, such as $Nd_2Fe_{14}B$, $SmCo_5$ as permanent magnets, $REFe_2$ as magneto-strictive devices and amorphous RE–(Fe, Co) as magneto-optical media [1–3]. Many research groups in the world are searching for new binary or ternary rare-earth and transition metal compounds. The investigation of new rare-earth containing compounds is interesting for both research and applications.

Melt spinning is a well known technique for fabrication of materials with amorphous and non-equilibrium phases. Many rare-earth containing materials prepared by melt spinning have shown excellent magnetic properties, such as high coercivity in $Nd_2Fe_{14}B$, $SmCo_5$ and amorphous RE–Fe alloys [1, 4, 5].

During our recent investigation of Nd–Fe–Al alloys, a ternary crystalline phase has been found, which exhibits metamagnetic behaviour at low temperatures. In this paper, we present the structural and magnetic characteristics of the ternary Nd–Fe–Al compound. The magneto-resistive results will be also reported.

2. Experimental details

The $Nd_{33}Fe_{50}Al_{17}$ ingot was prepared by arc melting. The ingot was crushed into small pieces for melt spinning. Three samples were prepared by melt spinning at different copper wheel surface speeds, 5, 15 and 30 m s^{-1}, respectively. Melt-spun ribbons were annealed at 873 K for 10 min under vacuum.

Melt-spun ribbons were examined using a differential scanning calorimeter (DSC) to study possible phase transformations. X-ray diffraction (Philips 1000 XRD with Cu Kα radiation) and transmission electron microscopy (TEM) were used for structural characterization.

0953-8984/99/5010557+10$30.00

An Oxford Instruments superconducting vibrating sample magnetometer (VSM) was used for the magnetic measurements in the temperature range of 4.2 to 290 K with a maximum magnetic field of 9 T. Magneto-resistance was measured in the VSM cryostat using a four point technique. Annealed ribbons were studied with a Ranger M-1200 ^{57}Fe-Mössbauer spectrometer at different temperatures between 78 and 290 K. A standard pure bcc-Fe foil was used for the calibration; therefore the chemical shift reported in this paper is relative to α-Fe.

3. Results

3.1. Structure

Figure 1 shows XRD patterns of ribbons melt spun at different wheel surface speeds. The ribbon melt spun at 30 m s^{-1} is amorphous. Crystalline peaks are seen in the XRD patterns of the ribbons melt spun at 15 and 5 m s^{-1} respectively. The ribbons were studied with differential scanning calorimetry (DSC). The crystallization temperature of the ribbon melt spun at 30 m s^{-1} was estimated to be 873 $\pm$ 10 K. A relatively large exothermic peak corresponding to crystallization was also present in the DSC curve of the ribbon melt spun at 15 m s^{-1}, indicating the presence of amorphous phase in the ribbon. The exothermic peak became much smaller for the ribbon melt spun at 5 m s^{-1}, showing a strong reduction of the amount of the amorphous phase.

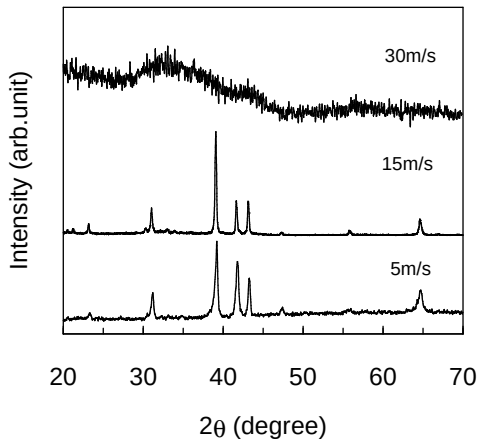

Figure 1. X-ray diffraction patterns of the ribbons melt spun at 5, 15 and 30 m s^{-1}, respectively.

Figure 2 shows XRD patterns of the three ribbons (melt spun at 5, 15 and 30 m s^{-1} respectively) after annealing at 873 K for 10 min. After crystallization, the diffraction peaks of the ribbon melt spun at 30 m s^{-1} can be identified as a mixture of a tetragonal phase and a small amount of hexagonal Nd. The lattice parameters of the tetragonal phase were $a = 9.778$ Å and $c = 11.516$ Å. The x-ray pattern of the annealed ribbon melt spun at 30 m s^{-1} is identical to the pattern of the crushed powder, showing that the ribbon is isotropic. For the ribbons melt spun at 15 m s^{-1}, the annealed ribbon possesses a crystallographic texture, as the (005) peak of the tetragonal phase has a higher intensity than the major (213) peak, indicating that c-axes of crystallites are predominantly perpendicular to the ribbon surface. The texture in the annealed ribbon melt spun at 5 m s^{-1} is stronger, as the intensity ratio of (005)/(213) is higher.

There are two peaks in the range of 40–45° that cannot be identified with the known Nd–Fe–Al phases [6, 17] in the XRD patterns of ribbons melt spun at 15 and 5 m s^{-1}

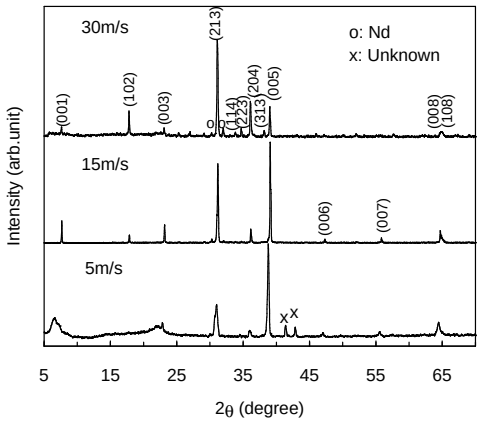

Figure 2. X-ray diffraction patterns of the ribbons melt spun at 5, 15 and 30 m s^{-1} and subsequently annealed at 873 K for 10 min.

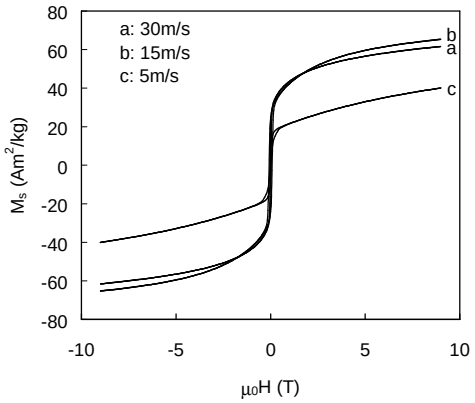

Figure 3. Hysteresis loops of the ribbons melt spun at 30 (a), 15 (b) and 5 m s^{-1} (c).

respectively (figure 1). This result indicates the presence of an unidentified phase coexisting with the tetragonal phase and crystalline Nd. After annealing at 873 K for 10 min, the two peaks disappear in the ribbon melt spun at 15 m s^{-1}, as shown in figure 2. The intensities of the two peaks are strongly reduced in the ribbon melt spun at 5 m s^{-1} after annealing at 873 K for 10 min. These results have shown that the unidentified phase is probably a metastable phase, which is formed during rapid quenching.

3.2. Magnetic measurements

Figure 3 shows hysteresis loops of melt spun ribbons. The ribbon melt spun at 30 m s^{-1} is magnetic and has a magnetization of 60 A m^2 kg^{-1} at the maximum field of 9 T. This result shows that the amorphous phase is magnetic at room temperature. As will be shown below, all the crystalline phases after crystallization are paramagnetic at room temperature. The ribbon melt spun at 15 m s^{-1} exhibits magnetic hysteresis and possesses a magnetization of 55 A m^2 kg^{-1} at 9 T, showing that a significant amount of the magnetic amorphous phase is present in the sample. After melt spinning at 5 m s^{-1}, the magnetization is

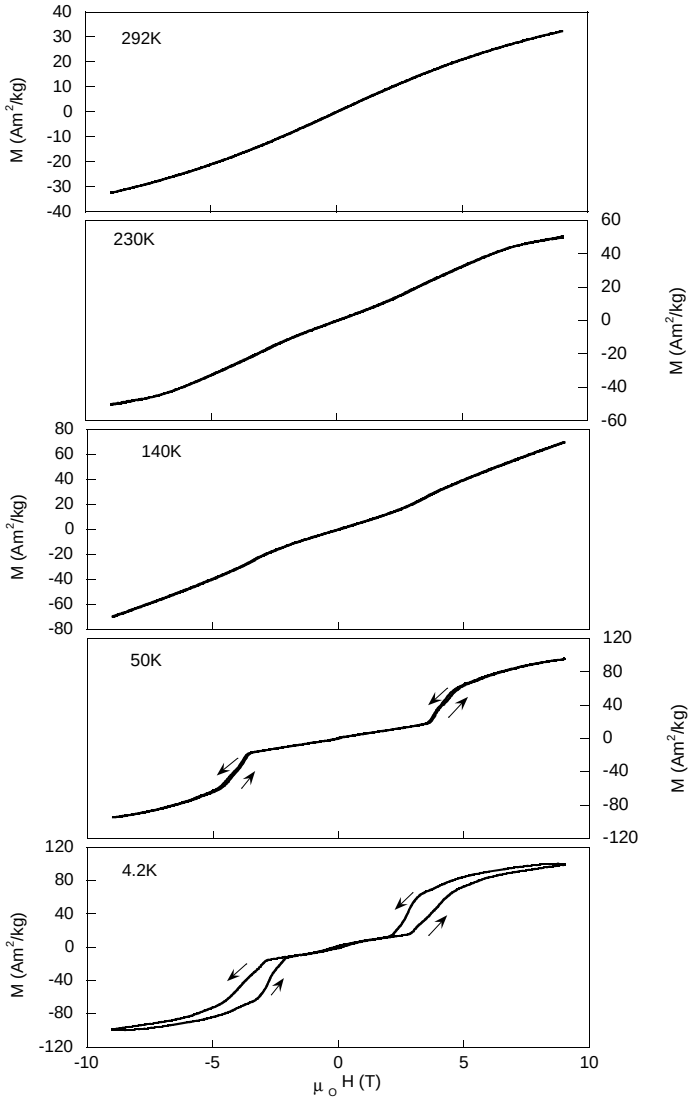

Figure 4. Magnetization curves taken at different temperatures for the ribbon melt spun at 30 m s^{-1} and subsequently annealed at 873 K for 10 min.

strongly reduced, indicating reduction of the amorphous phase because of the lower quenching rate.

After crystallization at 873 K, all the ribbons contain nearly the single tetragonal phase. The tetragonal phase is a new ternary Nd–Fe–Al phase according to our knowledge. In this work, magnetic and magneto-resistive properties of the new compound have been studied. Figure 4 shows magnetization curves at different temperatures for the annealed ribbon melt spun at 30 m s^{-1}. The room temperature curve exhibits paramagnetism. The magnetization curves taken at lower temperatures are as expected for antiferromagnetism. Figure 5 is the plot of inverse initial susceptibility versus temperature. A clear minimum of $1/\chi$ appears at 260 K. The minimum corresponds to the Néel temperature of the antiferromagnetic phase.

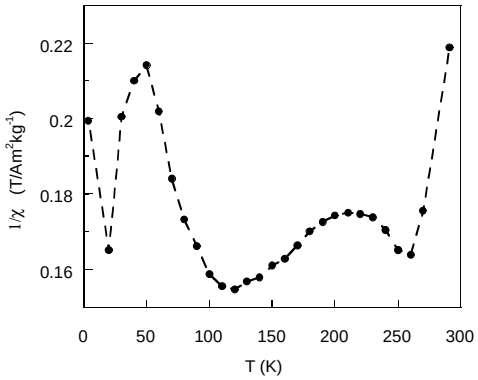

Figure 5. Inverse initial susceptibility ($1/\chi$) versus temperature (T).

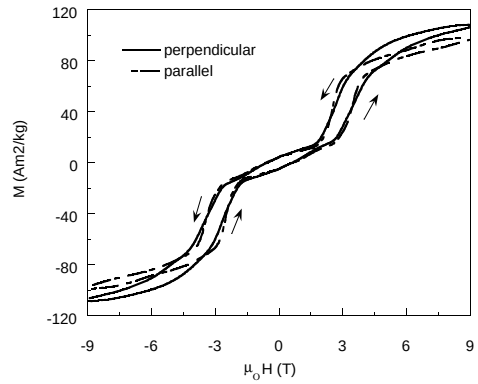

Figure 6. Magnetization curves measured in the two directions (perpendicular and parallel to the ribbon plane) for the ribbon melt spun at 5 m s^{-1} and annealed at 873 K for 10 min.

The tetragonal $Nd_{33}Fe_{50}Al_{17}$ compound exhibits metamagnetism at lower temperatures. In the magnetization curve measured at 140 K (figure 4), there is a small step in the field range of 3–4 T, indicating metamagnetism. The step increased with decreasing temperature. The transformation from antiferromagnetic coupling to ferromagnetic coupling is clearly shown in the magnetization curves taken at 50 and 4.2 K in figure 4. There is a significant hysteresis of the antiferro-/ferromagnetic coupling in the curve taken at 4.2 K.

The metamagnetic behaviour is related to the $1/\chi$ curve in figure 5. A broad minimum at around 120 K is associated with the appearance of metamagnetism. The fluctuation of $1/\chi$ below 50 K is probably related to the hysteresis, which is observed at a temperature of 50 K or below.

The annealed ribbon melt spun at 30 m s^{-1} is isotropic, i.e. the magnetization curves taken at different orientations (perpendicular or parallel to the ribbon plane) were the same. As shown above, a crystallographic texture was observed in ribbons melt spun at 15 and 5 m s^{-1} respectively. Figure 6 shows the magnetization curves taken in the perpendicular and parallel directions respectively for the annealed ribbon melt spun at 5 m s^{-1}. The magnetization in the perpendicular direction is approximately 10% higher. No significant difference in magnetization was found for the annealed ribbon melt spun at 15 m s^{-1}, by which the texture was strongly reduced as shown in figure 2.

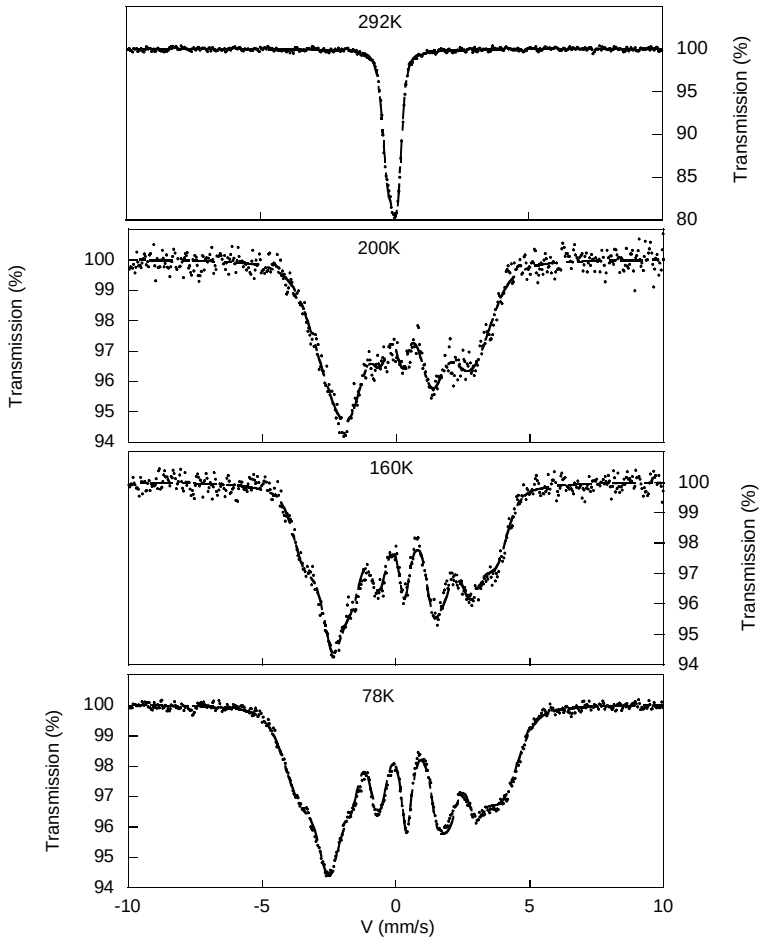

Figure 7. Mössbauer spectra taken at different temperatures for the ribbon melt spun at 30 m s^{-1} and subsequently annealed at 873 K for 10 min.

3.3. Mössbauer spectroscopy

The annealed ribbon melt spun at 30 m s^{-1} consisting nearly of the single tetragonal phase has been studied with ^{57}Fe-Mössbauer spectroscopy in this work. Figure 7 shows the Mössbauer spectra taken at different temperatures. The spectrum taken at 292 K is typical for a paramagnetic substance. The broad peak was fitted with a quadrupole splitting distribution as shown by the dashed line in figure 7, resulting in an average isomer shift of -0.07 mm s^{-1} and an average quadrupole splitting of 0.34 mm s^{-1}. Magnetic splitting is visible in the spectrum taken at 200 K or below, confirming the Néel temperature of 260 K measured using a magnetometer in figure 5. Broad peaks characterize all the Mössbauer spectra. For the spectrum taken at 78 K, at least eight sextets with a line width of 0.33 mm s^{-1} are required for the fitting (figure 7). The dashed lines in figure 7 represent the fitting of the hyperfine field distribution. The average hyperfine field increases with decreasing temperature, 16.7 T at 200 K, 18.5 T at 160 K and 20.6 T at 78 K.

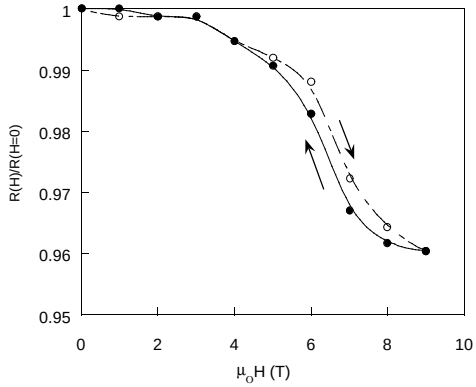

Figure 8. Magneto-resistance ($R(H)/R(H = 0)$) versus magnetic field ($\mu_0 H$) at 78 K for the ribbon melt spun at 30 m s^{-1} and annealed at 873 K.

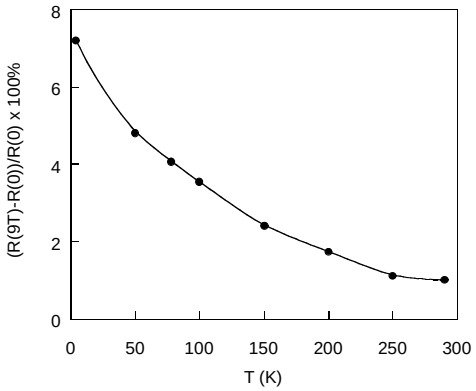

Figure 9. The maximum magneto-resistance ($(R(9\ \mathrm{T}) - R(0))/R(0) \times 100\%$) measured at 9 T versus temperature T for the ribbon melt spun at 30 m s^{-1} and annealed at 873 K.

3.4. Magneto-resistivity

In this work, magneto-resistivity has been studied for the annealed samples consisting of the tetragonal phase. Figure 8 shows the resistivity versus magnetic field at 78 K. A relatively rapid decrease of resistivity is observed in the field range of 4–6 T. This is certainly associated with the metamagnetism in the magnetization curve. A small hysteresis is found in the resistivity curve. A maximum magneto-resistivity of 4.1% is measured at 9 T (figure 8).

The maximum magneto-resistivity (measured at 9 T) is plotted as a function of temperature in figure 9. The maximum magneto-resistivity increases with decreasing temperature. At 4.2 K, the magneto-resistivity is 7.2%. At lower temperatures (<80 K), there is always a hysteresis present in the resistivity versus magnetic field curve. The hysteresis becomes larger with decreasing temperature. The hysteresis is certainly associated with the hysteresis observed in the magnetization curves (figure 6).

At room temperature (292 K), there is a magneto-resistivity of 1.0%, when the sample is in the paramagnetic state.

4. Discussion

Grieb [6] has summarized all the binary and ternary phases in the Nd–Fe–Al system. Comparing the structure and magnetic properties of the tetragonal phase in this work with those of the binary and ternary Nd–Fe–Al phases, the stable δ-$Nd_3Fe_{7-x}Al_x$ phase with $x = 0.8$–2.5 is the most similar phase. The δ phase has a tetragonal structure with $a = 8.10$ Å and $c = 23.10$ Å. However, a few diffraction peaks in figure 2, especially the (102) peak, cannot be identified with the δ phase.

Hu *et al* [7] have studied the δ phase with the composition of $Nd_6Fe_{11}Al_3$, which is very close to the composition of $Nd_{33}Fe_{50}Al_{17}$ in this work. The $Nd_6Fe_{11}Al_3$ compound is antiferromagnetic with a Néel temperature of 280–285 K, which is slightly higher than the Néel temperature of 260 K in this work. Metamagnetism has been found for the $Nd_6Fe_{11}Al_3$ compound at very low temperature (6 K) [7]. However, the magnetization of the $Nd_6Fe_{11}Al_3$ compound is much lower than the magnetization in figures 4 and 6. In addition, the Mössbauer spectra of the $Nd_6Fe_{11}Al_3$ compound could be well fitted with four well defined sextets. The Mössbauer spectra in figure 7 cannot be fitted with four sextets. The curves are much broader than the Mössbauer spectra in [7].

In a separate study, ribbons melt spun at 30, 15 and 5 m s^{-1} respectively were annealed at 873 K for 24 h. The XRD patterns of the annealed ribbons are very similar to the XRD pattern reported for the δ phase. In addition, the Néel temperature reduced from 260 to 250 K, and the metamagnetism was reduced in comparison with the magnetization curves in figure 4 and 6. In figure 2, the (102) peak has a very low intensity in the ribbon melt spun at 5 m s^{-1} and subsequently annealed at 873 K. This ribbon may contain a certain amount of the stable δ phase.

All of the facts discussed above suggest that the tetragonal phase in this work is probably a metastable ternary Nd–Fe–Al phase, which has a composition very close to Nd_2Fe_3Al. This phase has a structure which is related to the stable δ phase. The different Néel temperature, broadened Mössbauer spectra and more significant metamagnetism are probably due to a structural disorder in comparison with the stable δ phase. The tetragonal Nd_2Fe_3Al phase is formed after crystallization from amorphous or directly during quenching.

The average hyperfine field of the $Nd_6Fe_{11}Al_3$ compound is 23.7 T [7]. The $Nd_{33}Fe_{51}Al_{17}$ alloy in this work has an average hyperfine field of 20.6 T at 77 K. These results indicate that the two phases have similar values of Fe magnetic moments.

Metamagnetism has been reported in many systems, such as $MnAu_2$, $RECu_2$, $RE_3Fe_{7-x}M_x$ with M = Al, Ge or Si [7–9]. The antiferro-/ferromagnetic transformation is in many cases strongly dependent on crystallographic orientation, i.e. the metamagnetism is observed in certain crystallographic axes [9]. The metamagnetism in the tetragonal Nd_2Fe_3Al compound is nearly isotropic, as no significant difference in magnetization is found between isotropic and anisotropic samples (figures 4 and 6).

Taking the expected average hyperfine field of 23 T for Fe atoms at 4.2 K [7], the average magnetic moment is 1.5 μ_B per iron using 15 T μ_B^{-1} as the proportionality constant of the ratio of hyperfine field/magnetic moment. Assuming the magnetic moment of Nd is 3.3 μ_B [10] and $\mu_{Al} = 0$, the calculated magnetization is 125 A m^2 kg^{-1}, if all Nd and Fe moments are ferromagnetically coupled. The maximum magnetization at 9 T is 100 A m^2 kg^{-1} at 4.2 K (figure 4). This result indicates that the magnetization of the Nd_2Fe_3Al compound is not far below the ferromagnetic saturation at the magnetic field of 9 T at 4.2 K.

Magneto-resistivity or giant magneto-resistivity (GMR) has been reported in many systems including coupled and non-coupled multi-layers [11, 12]. GMR has been observed in granular

Co–Cu or Fe–Cu based on superparamagnetism [13, 14]. Recently, GMR has been found in compounds with layered antiferromagnetic structure, such as $SmMn_2Ge_2$ and FeRh [15, 16]. The GMR effect in $SmMn_2Ge_2$ and FeRh is due to the antiferro-/ferromagnetic transformation. The magneto-resistivity in $Nd_{33}Fe_{50}Al_{17}$ ribbons in this work is certainly associated with the metamagnetic behaviour. The change of antiferromagnetic to ferromagnetic coupling at lower temperatures may lead to a reduction of resistivity.

In this work, magneto-resistivity of 1% is also found at room temperature in the paramagnetic state. This is a phenomenon which has not been reported before to our knowledge. The sample has a fairly high maximum magnetization of 32 A m^2 kg^{-1} at room temperature (figure 4). The high magnetization indicates a high degree of magnetic alignment at 292 K, which is not far below the Néel temperature (260 K). Since the metastable Nd_2Fe_3Al phase probably has a disordered structure as shown by the Mössbauer spectra (figure 7), inhomogeneities or clusters may be present. Magneto-resistivity related with inhomogeneities or clusters has been reported in many systems [13, 14]. Our future work will be concentrated on the investigation of the origin of the magneto-resistivity in the Nd_2Fe_3Al and other related compounds.

5. Conclusion

An amorphous phase can be formed in $Nd_{33}Fe_{50}Al_{17}$ after melt spinning at 30 m s^{-1}, while crystalline phases are present at lower wheel surface speeds. The amorphous phase crystallizes into a mixture of a tetragonal phase and a small amount of Nd. The tetragonal phase has lattice parameters of $a = 9.778$ Å and $c = 11.516$ Å. The tetragonal phase is probably a metastable phase and slowly transforms into the stable δ-$Nd_3Fe_{7-x}Al_x$ phase [7].

The tetragonal phase is an antiferromagnetic phase with a Néel temperature of 260 K. Metamagnetic behaviour is observed at a temperature of 140 K or below. At 4.2 K, the magnetization measured at 9 T is not far below the theoretical magnetization assuming ferromagnetic coupling of all the Nd and Fe moments.

Magneto-resistivity is present in the $Nd_{33}Fe_{50}Al_{17}$ compound. At lower temperatures ($<$120 K), magneto-resistivity is associated with metamagnetism, since a rapid decrease of resistivity is observed after the antiferro-/ferromagnetic transformation. Magneto-resistivity increases with decreasing temperature, from 4.1% at 78 K to 7.2% at 4.2 K. 1% of magneto-resistivity is estimated at room temperature in the paramagnetic state. This phenomenon is to be further investigated.

References

[1] Buschow K H J 1998 *Ferromagnetic Materials* vol 4, ed E P Wohlfarth and K H J Buschow (Amsterdam: Elsevier) p 1
[2] Pinkerton F E, Capehart T W, Herbst J F, Brewer E G and Murphy B C 1997 *Appl. Phys. Lett.* **70** 2601
[3] Kim M J, Bow J S, Carpenter R W and Liu J 1994 *IEEE Trans. Magn.* **30** 4398
[4] Croat J J 1982 *IEEE Trans. Magn.* **18** 1442
[5] Croat J J 1981 *J. Appl. Phys.* **52** 2509
[6] Grieb B 1994 *Ternary Alloys* vol 5, ed G Pethow and G Effenberg (New York: VCH)
[7] Hu B P and Coey J M D 1992 *J. Magn. Magn. Mater.* **225–231** 117
[8] Meyer A J P and Taylang P 1956 *J. Physique Radium* **17** 457
[9] Luong N H and Franse J J M 1995 *Handbook of Magnetic Materials* vol 8, ed K H J Buschow (Amsterdam: Elsevier) p 415
[10] Chikazumi S 1964 *Physics of Magnetism* (Malabar, FL: Krieger)
[11] Shinjo T and Ono T 1998 *J. Magn. Magn. Mater.* **177–181** 31
[12] Birach G, Grunberg P, Saurenbach F and Zinn W 1989 *Phys. Rev.* B **39** 4828

[13] Wecker J, von Helmolt R, Schultz L and Samwer K 1993 *Appl. Phys. Lett.* **62** 1985
[14] Ding J, Eilon M, Street R, St Pierre T, Smith P and McCormick P G 1995 *J. Magn. Magn. Mater.* **140–144** 471
[15] van Dover R B, Gyorgy E M, Cava R J, Krajevski J J, Felder R J and Peck W F 1993 *Phys. Rev.* B **47** 6134
[16] Algarabel R A, Ibarra M R, Marquina C, del Moral A, Galibert J, Iqqbal M and Askenazy S 1995 *Appl. Phys. Lett.* **66** 3062
[17] Ding J, Si L, Li Y and Wang X Z 1999 *Appl. Phys. Lett.* **75** 1763